Since January 2020 Elsevier has created a COVID-19 resource centre with free information in English and Mandarin on the novel coronavirus COVID-19. The COVID-19 resource centre is hosted on Elsevier Connect, the company's public news and information website.

Microbial Risk Analysis 23 (2023) 100249

Contents lists available at ScienceDirect

Microbial Risk Analysis

journal homepage: www.elsevier.com/locate/mran

The SARS-CoV-2 Hydra, a tiny monster from the 21st century: Thermodynamics of the BA.5.2 and BF.7 variants

Marko Popovic

School of Life Sciences, Technical University of Munich, 85354 Freising, Germany

ARTICLE INFO

Keywords:
COVID-19
Variant of concern
Infectivity
Pathogenicity
Evolution
Gibbs energy

ABSTRACT

SARS-CoV-2 resembles the ancient mythical creature Hydra. Just like with the Hydra, when one head is cut, it is followed by appearance of two more heads, suppression of one SARS-CoV-2 variant causes appearance of newer variants. Unlike Hydra that grows identical heads, newer SARS-CoV-2 variants are usually more infective, which can be observed as time evolution of the virus at hand, which occurs through acquisition of mutations during time. The appearance of new variants is followed by appearance of new COVID-19 pandemic waves. With the appearance of new pandemic waves and determining of sequences, in the scientific community and general public the question is always raised of whether the new variant will be more virulent and more pathogenic. The two variants characterized in this paper, BA.5.2 and BF.7, have caused a pandemic wave during the late 2022. This paper gives full chemical and thermodynamic characterization of the BA.5.2 and BF.7 variants of SARS-CoV-2. Having in mind that Gibbs energy of binding and biosynthesis represent the driving forces for the viral life cycle, based on the calculated thermodynamic properties we can conclude that the newer variants are more infective than earlier ones, but that their pathogenicity has not changed.

1. Introduction

"*Hydra, that monster with a ring of heads with power to grow again*" [Euripides, 2023]. The Hydra of Lerna is an epic monster from Greek mythology. It was mentioned for the first time by Hesiod in his poem Theogony, composed between 730 and 700 BC [Hesiod, 2023]. Hydra was said to be a gigantic water-snake-like monster with multiple heads [Britannica, 2023]. It was believed to live in the marshes of Lerna, near Árgos [Britannica, 2023]. Hydra has an ability of regeneration – when one head is cut off, two more grow to take its place [Euripides, 2023; Britannica, 2023]. Hydra, the monster of our imagination, has come to haunt us in the 21st century in the form of a virus. SARS-CoV-2 has multiple variants. Each variant brings a new pandemic wave. Every time a variant is suppressed, one or more variants appear to take its place.

Living organisms represent open thermodynamic systems, which during interactions with their animate and inanimate surroundings change their thermodynamic parameters [Boltzmann, 1974; von Bertalanffy, 1950, 1971; Balmer, 2010; Popovic, 2018a, 2018b; Prigogine and Wiame, 1946; Prigogine, 1977, 1947; Glansdorff and Prigogine, 1971; Morowitz et al., 2000, 1988; Morowitz, 1995, 1992, 1976, 1968, 1955; Schrödinger, 1944; Ozilgen and Sorgüven, 2017]. Even though they represent the simplest biological systems, viruses completely fit into von Bertalanffy's theory of open systems in biology [von Bertalanffy, 1950, 1971].

Viruses are obligate intracellular parasites, which hijack metabolism and resources of their host cells, and use their host cell to perform basic biological functions [Popovic and Minceva, 2020a, 2020b]. Until 2019, the empirical formula was known only for the poliovirus [Wimmer, 2006; Molla et al., 1991]. Since the beginning of the COVID-19 pandemic, there has been an intense development of biothermodynamics of viruses. The next virus to be chemically and thermodynamically characterized was the Hu-1 variant of SARS-CoV-2 [Popovic, 2022a]. During the COVID-19 pandemic, SARS-CoV-2 has mutated many times on the genes encoding the spike glycoprotein and other viral proteins. The consequence of mutations was development of new variants. Chemical and thermodynamic characterization of new virus variants has been reported in the literature [Popovic and Popovic, 2022; Özilgen and Yilmaz, 2021; Yilmaz et al., 2020; Nadi and Özilgen, 2021; Şimşek et al., 2021; Degueldre, 2021; Popovic, 2022a, 2022b, 2022c, 2022d, 2022e, 2022f, 2022g, 2022h, 2022i, 2022j; Gale, 2022; Lucia, 2021, 2020a, 2020b; Kaniadakis et al., 2020; Popovic and Minceva, 2021a, 2020b; Istifli et al., 2022]. In that way, biothermodynamics has followed the reports on sequencing of nucleic acids and proteins of various variants. The atom counting method has been developed, which

E-mail address: marko.popovic@tum.de.

https://doi.org/10.1016/j.mran.2023.100249
Received 8 January 2023; Received in revised form 1 February 2023; Accepted 1 February 2023
Available online 4 February 2023

determines empirical formulas of viruses, based on their genetic and protein sequences [Popovic, 2022k].

Thermodynamic analysis and calorimetry have for a long time been used in research on viruses. The calorimetric methods include differential scanning calorimetry (DSC), isothermal titration calorimetry (ITC) and reaction calorimetry (isothermal microcalorimetry) [Privalov, 2012; Sarge et al., 2014]. Differential scanning calorimetry (DSC) has been applied to measure energetics of virus capsid self-assembly and denaturation [Krell et al., 2005; Yang et al., 2017], virus particle structure [Bauer et al., 2015, 2013], thermal stability [Yang et al., 2017; Makarov et al., 2013; Virudachalam et al., 1985a, 1985b], virus identification [Krell et al., 2005], virus denaturation [Toinon et al., 2015 ; Brouillette et al., 1982], entry into host cell [Banerjee et al., 2010; Nebel et al., 1995], capsid self-assembly [Sturtevant et al., 1981; Stauffer, 1970] and vaccine development [Deschuyteneer et al., 2010; Wang et al., 2015].

Isothermal titration calorimetry (ITC) was also applied to study a wide range of phenomena related to viruses, such as virus adsorption and disassembly [Yu et al., 2015], influence on metabolism and cell cycle [Javorsky et al., 2022; Prins et al., 2010], apoptosis inhibition [Anasir et al., 2017; Aladag et al., 2014], virus structure and entry into host cells [Liu et al., 2014], nucleocapsid self-assembly [Maassen et al., 2019], inactivation [Yang et al., 2020; Kawahara et al., 2018], immune response evasion [Gao et al., 2021], antiviral therapy development [Zhou et al., 2022; Noble et al., 2016; Sharma et al., 2016; Byrn et al., 2015] and vaccine development [Vorobieva et al., 2014].

Reaction calorimetry (isothermal microcalorimetry) has been applied to study virus multiplication inside host cells [Sigg et al., 2022; Tkhilaishvili et al., 2018a; Guosheng et al., 2003; Morais et al., 2014], phage action against bacterial biofilms [Tkhilaishvili et al., 2020a, 2020b, 2018a, 2018b, 2018c; Wang et al., 2020a, 2020b; Tkhilaishvili et al., 2018b], phage-bacteria interactions [Fanaei Pirlar et al., 2022; Wang et al., 2020c], phage transition from lytic into lysogenic cycles [Maskow et al., 2010], antiviral therapy [Shadrick et al., 2013; Tkhilaishvili, 2022; Gelman et al., 2021], and influence on marine ecosystem metabolism [Djamali et al., 2012].

Working with SARS-CoV-2 requires a high biosafety level and few analytic and biothermodynamic laboratories fulfill such conditions. To overcome this obstacle, the atom counting method was developed [Popovic, 2022k], which proved itself useful in chemical and thermodynamic characterization of contagious viruses like SARS-CoV-2. During the last year, the atom counting method has proved itself useful in characterization of other viruses, including Ebola [Popovic, 2022j], Monkeypox [Popovic, 2022L], Herpes [Popovic, 2022m], HIV-1 [Popovic, 2022n] and bacteriophages [Popovic, 2022q], as well as viroids [Popovic, 2023].

Change in thermodynamic properties represents the driving force for most processes in nature [Demirel, 2014; Balmer, 2010; Atkins and de Paula, 2011, 2014; Ozilgen and Sorgüven, 2017]. The viral life cycle consists of several processes, which have their biological, chemical and thermodynamic nature [Popovic, 2022i, 2022p, Ridgway et al., 2022]. Replication of viral nucleic acid represents a chemical reaction of polymerization of nucleotides driven by Gibbs energy of biosynthesis [Dodd et al., 2020; Johansson and Dixon, 2013]. Transcription represents a polymerization reaction that produces mRNA [Pinheiro et al., 2008]. Translation represents a chemical reaction of polymerization of amino acids into proteins [Popovic, 2022i; Lee et al., 2020]. Virus binding represents a chemical reaction similar to protein ligand interaction, driven by Gibbs energy of binding [Gale, 2021, 2020, 2019, 2018]. Self-assembly of viral components represents a physical process, also led by changes in thermodynamic properties [Katen and Zlotnick, 2009; Maassen et al., 2019].

The goal of this paper is to perform a chemical and thermodynamic characterization of the BA.5.2 and BF.7 variants of SARS-CoV-2, to estimate their infectivity and pathogenicity, which depend on kinetic (e.g. biosynthesis rate and binding rate) and thermodynamic properties (e.g. enthalpy, entropy and Gibbs energy).

2. Methods

2.1. Data sources

The genetic sequences of the BA.5.2 and BF.7 variants of SARS-CoV-2 were taken from GISAID, the global data science initiative [Khare et al., 2021; Elbe and Buckland-Merrett, 2017; Shu and McCauley, 2017]. The genetic sequence of the BA.5.2 isolate from Australia is labeled hCoV-19/Australia/NSW-ICPMR-40038/2022. It can be found under the accession ID: EPI_ISL_16342181. It was isolated in Sydney on December 18, 2022. It was sequenced using Illumina technology. The genetic sequence of the BA.5.2 isolate from Japan is labeled hCoV-19/Japan/PG-416497/2022. It can be found under the accession ID: EPI_ISL_16374653. It was isolated in Fukuoka on December 3, 2022. It was sequenced using Illumina MiSeq technology. The genetic sequence of the BA.5.2 isolate from USA is labeled hCoV-19/USA/NH-CDC-LC0969162/2022. It can be found under the accession ID: EPI_ISL_16382809. It was isolated in New Hampshire on December 23, 2022. It was sequenced using PacBio Sequel II technology. The genetic sequence of the BF.7 isolate from China is labeled hCoV-19/Beijing/CPL-12-64/2022. It can be found under the accession ID: EPI_ISL_16348517. It was isolated in Beijing on December 19, 2022. It was sequenced using Illumina NextSeq technology. The genetic sequence of the BF.7 isolate from Greece is labeled hCoV-19/Greece/345194/2022. It can be found under the accession ID: EPI_ISL_16383259. It was isolated in Attica on November 17, 2022. It was sequenced using Illumina NovaSeq 6000 technology. The genetic sequence of the BF.7 isolate from Serbia is labeled hCoV-19/Serbia/K563312-11/2022. It can be found under the accession ID: EPI_ISL_16317088. It was isolated in Belgrade on November 21, 2022. It was sequenced using MGI-DNBSEQ technology. Therefore, the findings of this study are based on metadata associated with 6 sequences available on GISAID up to January 7, 2023, and accessible at https://doi.org/10.55876/gis8.230107ef

The sequence of the nucleocapsid phosphoprotein of SARS-CoV-2 was obtained from the NCBI database [Sayers et al., 2022; National Center for Biotechnology Information, 2022], under the accession ID: UKQ14424.1. The number of copies of the nucleocapsid phosphoprotein in virus particle was taken from [Neuman and Buchmeier, 2016; Neuman et al., 2011; Neuman et al., 2006]. In a SARS-CoV-2 particle, there are 2368 copies of the nucleocapsid phosphoprotein [Neuman and Buchmeier, 2016; Neuman et al., 2011; Neuman et al., 2006].

The dissociation equilibrium constant, K_d, of the spike glycoprotein of BF.7 variant of SARS-CoV-2 to the human ACE2 receptor was taken from [Wang et al., 2022]. Its value is $K_d = 0.4$ nM [Wang et al., 2022]. It was measured using surface plasmon resonance at 25°C [Wang et al., 2022].

2.2. Empirical formulas and biosynthesis reactions

The genetic and protein sequences were used to find empirical formulas of nucleocapsids of the BA.5.2 and BF.7 variants of SARS-CoV-2. This was done using the atom counting method [Popovic, 2022k]. The atom counting method is implemented using a computer program [Popovic, 2022k]. The input are genetic and protein sequences of the virus of interest, as well as the number of copies of proteins in the virus particle and the virus particle size [Popovic, 2022k]. The program goes along the nucleic acid and protein sequences and adds atoms coming from each residue in the sequence, to find the number of atoms contributed by that macromolecule to the virus particle [Popovic, 2022k]. The contributions of viral proteins are multiplied by their copy numbers, since proteins are present in multiple copies in virus particles [Popovic, 2022k]. The output of the program is elemental composition of virus particles, in the form of empirical formulas, and molar masses of virus particles [Popovic, 2022k]. The advantage of the atom counting method is that it can provide the empirical formulas of virus particles,

based on widely available data on genetic and protein sequences [Popovic, 2022k]. The atom counting method was shown to give results in good agreement with experimental results [Popovic, 2022k].

The empirical formulas of virus particles were used to construct biosynthesis reactions, summarizing conversion of nutrients into new live matter [von Stockar, 2013a, 2013b; Battley, 1998]. The biosynthesis reaction for virus particles has the general form

$$(Amino\ acid) + O_2 + HPO_4^{2-} + HCO_3^- \rightarrow (Bio) + SO_4^{2-} + H_2O + H_2CO_3 \quad (1)$$

where (Bio) represents new live matter, described by an empirical formula given by the atom counting method [Popovic, 2022b, 2022c, 2022f]. (Amino acid) represents a mixture of amino acids with the empirical formula $CH_{1.798}O_{0.4831}N_{0.2247}S_{0.022472}$ (expressed per mole of carbon), representing the source of energy, carbon, nitrogen and sulfur [Popovic, 2022b, 2022c, 2022f]. O_2 is the electron acceptor [Popovic, 2022b, 2022c, 2022f]. HPO_4^{2-} is the source of phosphorus [Popovic, 2022b, 2022c, 2022f]. HCO_3^- is a part of the bicarbonate buffer that takes excess H^+ ions that are generated during biosynthesis [Popovic, 2022b, 2022c, 2022f]. SO_4^{2-} is an additional metabolic product that takes excess sulfur atoms [Popovic, 2022b, 2022c, 2022f]. H_2CO_3 takes the oxidized carbon atoms and is also a part of the bicarbonate buffer [Popovic, 2022b, 2022c, 2022f].

2.3. Thermodynamic properties of live matter and biosynthesis

Empirical formulas of virus nucleocapsids were used to find standard thermodynamic properties of their live matter, using predictive biothermodynamic models: the Patel-Erickson and Battley equations [Patel and Erickson, 1981; Battley, 1999, 1998, 1992]. The Patel-Erickson equation was used to find enthalpy of live matter, based on its elemental composition. The Patel-Erickson equation gives standard enthalpy of combustion, $\Delta_C H^o$, of live matter

$$\Delta_C H^0(bio) = -111.14 \frac{\text{kJ}}{\text{C}-\text{mol}} E \quad (2)$$

where E is number of electrons transferred to oxygen during combustion [Patel and Erickson, 1981; Battley, 1998, 1992]. E can be calculated from the empirical formula of live matte

$$E = 4n_C + n_H - 2n_O - 0\ n_N + 5n_P + 6n_S \quad (3)$$

where n_C, n_H, n_O, n_N, n_P and n_S represent the numbers of C, H, O, N, P and S atoms in the live matter empirical formula, respectively [Patel and Erickson, 1981; Battley, 1998, 1992]. Once calculated using the Patel-Erickson equation, $\Delta_C H^o$ can be converted into standard enthalpy of formation, $\Delta_f H^o$, of live matter. $\Delta_C H^o$ is the enthalpy change of the reaction of complete combustion of live matter.

$$C_{nC}H_{nH}O_{nO}N_{nN}P_{nP}S_{nS} + (n_C + 1/4n_H + 11/4n_P + 11/2n_S - 1/2n_O)O_2 \rightarrow n_C CO_2 + 1/2n_H H_2O + 1/2n_N N_2 + 1/4n_P P_4O_{10} + n_S SO_3 \quad (4)$$

This means that $\Delta_C H^o$ can be used to find $\Delta_f H^o$ of live matter using the equation [Popovic, 2022b, 2022c, 2022f; Atkins and de Paula, 2011, 2014]

$$_fH^0(bio) = n_C \Delta_f H^0(CO_2) + \frac{n_H}{2} \Delta_f H^0(H_2O) + \frac{n_P}{4} \Delta_f H^0(P_4O_{10}) + n_S \Delta_f H^0(SO_3) - \Delta_C H^0 \quad (5)$$

The Battley equation gives standard molar entropy of live matter, S^o_m, based on its empirical formula

$$S^0_m(bio) = 0.187 \sum_J \frac{S^0_m(J)}{a_J} n_J \quad (6)$$

where n_J is the number of atoms of element J in the empirical formula of live matter [Battley, 1999; Battley and Stone, 2000]. S^o_m and a_J are standard molar entropy and number of atoms per formula unit of element J in its standard state elemental form [Battley, 1999; Battley and Stone, 2000]. The Battley equation can be modified to give standard entropy of formation, $\Delta_f S^o$, of live matter [Battley, 1999; Battley and Stone, 2000]

$$S^0_m(bio) = -0.813 \sum_J \frac{S^0_m(J)}{a_J} n_J \quad (7)$$

Finally, $\Delta_f H^o$ and $\Delta_f S^o$ are combined to give standard Gibbs energy of formation of live matter, $\Delta_f G^o$.

$$\Delta_f G^0(bio) = \Delta_f H^0(bio) - T\Delta_f S^0(bio) \quad (8)$$

Once live matter is characterized by finding its $\Delta_f H^o$, S^o_m and $\Delta_f G^o$, these properties can be combined with biosynthesis reactions to find standard thermodynamic properties of biosynthesis. Standard thermodynamic properties of biosynthesis include standard enthalpy of biosynthesis, $\Delta_{bs}H^o$, standard entropy of biosynthesis, $\Delta_{bs}S^o$, and standard Gibbs energy of biosynthesis, $\Delta_{bs}G^o$. These properties are found by applying the Hess's law to biosynthesis reactions

$$\Delta_{bs}H^0 = \sum_{products} \nu\ \Delta_f H^0 - \sum_{reactants} \nu\ \Delta_f H^0 \quad (9)$$

$$\Delta_{bs}S^0 = \sum_{products} \nu\ S^o_m - \sum_{reactants} \nu\ S^o_m \quad (10)$$

$$\Delta_{bs}G^0 = \sum_{products} \nu\ \Delta_f G^0 - \sum_{reactants} \nu \Delta_f G^0 \quad (11)$$

where ν represents a stoichiometric coefficient [Popovic, 2022b, 2022c, 2022f; Atkins and de Paula, 2011, 2014; von Stockar, 2013a, 2013b; Battley, 1998]. The most important of these three properties is standard Gibbs energy of biosynthesis, which represents the thermodynamic driving force for growth of all organisms [von Stockar, 2013a, 2013b; von Stockar and Liu, 1999], including viruses [Popovic, 2022b, 2022c, 2022f, 2022i].

2.4. Thermodynamic properties of antigen-receptor binding

In order to multiply inside the cytoplasm, a virus must first enter its host cell. The first step in this process is binding of the virus antigen to the host cell receptor. The antigen of SARS-CoV-2 is the spike glycoprotein trimer (SGP) [Duan et al., 2020], while the host cell receptor is angiotensin-converting enzyme 2 (ACE2) [Scialo et al., 2020]. The process of antigen-receptor binding is, in its essence, a chemical reaction, similar to protein-ligand interactions [Du et al., 2016; Popovic and Popovic, 2022]. Thus, the binding of SGP to ACE2 can be described through the chemical reaction

$$(An) + (Re) = (An - Re)$$

where (*An*) represents the virus antigen (SGP in the case of SARS-CoV-2), (*Re*) represents the host cell receptor (ACE2 for SARS-CoV-2), while (*An-Re*) represents the antigen-receptor complex [Du et al.,

Table 1
Empirical formulas of nucleocapsids of BA.5.2 and BF.7 variants of SARS-CoV-2 isolated in various countries. The empirical formula of live matter has the general form $C_{nC}H_{nH}O_{nO}N_{nN}P_{nP}S_{nS}$. In addition, molar masses were reported for the empirical formulas, *Mr*, and for entire nucleocapsids, *Mr*(*nc*).

Variant	C	H	O	N	P	S	Mr (g/mol)	Mr(nc) (MDa)
BA.5.2 nucleocapsid - Australia	1	1.573784	0.342390	0.312321	0.005956	0.003361	23.7419	117.0958
BA.5.2 nucleocapsid - Japan	1	1.573557	0.342676	0.312372	0.006022	0.003359	23.7489	117.2088
BA.5.2 nucleocapsid - USA	1	1.573566	0.342668	0.312369	0.00602	0.003359	23.7487	117.2050
BF.7 nucleocapsid - China	1	1.573531	0.342715	0.312374	0.006031	0.003358	23.7498	117.2227
BF.7 nucleocapsid - Greece	1	1.573511	0.342740	0.312379	0.006036	0.003358	23.7504	117.2326
BF.7 nucleocapsid - Serbia	1	1.573528	0.342718	0.312375	0.006031	0.003358	23.7499	117.2241

2016; Popovic and Popovic, 2022].

Like for all other chemical reactions, laws of chemical thermodynamics apply and the process of antigen-receptor binding can be described through several thermodynamic parameters. The dissociation equilibrium constant, K_d, is defined as

$$K_d = \frac{[An][Re]}{[An - Re]} \tag{12}$$

where [*An*] is the concentration of the virus antigen, [*Re*] the concentration of the host receptor and [*An-Re*] the concentration of the antigen-receptor complex [Du et al., 2016; Popovic and Popovic, 2022]. The reciprocal of K_d is the binding equilibrium constant, K_B, [Du et al., 2016; Popovic and Popovic, 2022]

$$K_B = \frac{1}{K_d} \tag{13}$$

The binding equilibrium constant can be used to find standard Gibbs energy of binding, $\Delta_B G^o$, through the equation

$$\Delta_B G^0 = -RT\ln K_B \tag{14}$$

Where T is temperature and R is the universal gas constant [Du et al., 2016; Popovic and Popovic, 2022].

2.5. Uncertainties

The Patel-Erickson equation gives $\Delta_C H^o$ values within 5.36 % accuracy [Popovic, 2019]. The uncertainty in the S^o_m values found through the Battley equation is 19.7 % or less [Battley, 1999a]. The uncertainties in $\Delta_C H^o$ and S^o_m values were used to find uncertainties in the final results for thermodynamic properties of live matter ($\Delta_f H^o$ and $\Delta_f G^o$) and thermodynamic properties of biosynthesis ($\Delta_{bs} H^o$, $\Delta_{bs} S^o$ and $\Delta_{bs} G^o$), through classical error propagation.

3. Results

Based on the dissociation equilibrium constant reported in the literature [Wang et al., 2022], standard Gibbs energy of binding of the BF.7 variant of SARS-CoV-2 was found to be -53.64 kJ/mol, at 25°C.

Based on genetic and protein sequences, elemental composition was determined for nucleocapsids of the BA.5.2 and BF.7 variants of SARS-CoV-2. It is reported in the form of empirical formulas, which are given in Table 1, together with their molar masses. The empirical formula of the BA.5.2 nucleocapsid isolated in Australia is $CH_{1.573784}O_{0.342390}N_{0.312321}P_{0.005956}S_{0.003361}$, with a molar mass of 23.7419 g/mol. The molar mass of the entire nucleocapsid of the BA.5.2 sample from Australia is 117.0958 MDa. The empirical formula of the BA.5.2 nucleocapsid isolated in Japan is $CH_{1.573557}O_{0.342676}N_{0.312372}P_{0.006022}S_{0.003359}$, with a molar mass of 23.7489 g/mol. The molar mass of the entire nucleocapsid of the BA.5.2 sample from Japan is 117.2088 MDa. The empirical formula of the BA.5.2 nucleocapsid isolated in USA is $CH_{1.573566}O_{0.342668}N_{0.312369}P_{0.00602}S_{0.003359}$, with a molar mass of 23.7487 g/mol. The molar mass of the entire nucleocapsid of the BA.5.2 sample from USA is 117.2050 MDa. The empirical formula of the BF.7 nucleocapsid isolated in China is $CH_{1.573531}O_{0.342715}N_{0.312374}P_{0.006031}S_{0.003358}$, with a molar mass of 23.7498 g/mol. The molar mass of the entire nucleocapsid of the BF.7 sample from China is 117.2227 MDa. The empirical formula of the BF.7 nucleocapsid isolated in Greece is $CH_{1.573511}O_{0.342740}N_{0.312379}P_{0.006036}S_{0.003358}$, with a molar mass of 23.7504 g/mol. The molar mass of the entire nucleocapsid of the BF.7 sample from Greece is 117.2326 MDa. The empirical formula of the BF.7 nucleocapsid isolated in Serbia is $CH_{1.573528}O_{0.342718}N_{0.312375}P_{0.006031}S_{0.003358}$, with a molar mass of 23.7499 g/mol. The molar mass of the entire nucleocapsid of the BF.7 sample from Serbia is 117.2241 MDa. Based on the empirical formulas, biosynthesis reactions were formulated and reported in Table 2.

Table 3 gives standard thermodynamic properties of live matter of nucleocapsids of the BA.5.2 and BF.7 variants of SARS-CoV-2. These include standard enthalpy of formation, $\Delta_f H^o$, standard molar entropy, S^o_m, and standard Gibbs energy of formation, $\Delta_f G^o$. For the nucleocapsid of the BA.5.2 isolate from Australia, standard enthalpy of formation is -75.32 kJ/C-mol, standard molar entropy is 32.49 J/C-mol K, and standard Gibbs energy of formation is -33.21 kJ/C-mol. For the nucleocapsid of the BA.5.2 isolate from Japan, standard enthalpy of formation is -75.39 kJ/C-mol, standard molar entropy is 32.49 J/C-mol K, and standard Gibbs energy of formation is -33.27 kJ/C-mol. For the nucleocapsid of the BA.5.2 isolate from USA, standard enthalpy of formation is -75.39 kJ/C-mol, standard molar entropy is 32.49 J/C-mol K, and standard Gibbs energy of formation is -33.27 kJ/C-mol. For the nucleocapsid of the BF.7 isolate from China, standard enthalpy of formation is -75.40 kJ/C-mol, standard molar entropy is 32.49 J/C-mol K, and standard Gibbs energy of formation is -33.28 kJ/C-mol. For the nucleocapsid of the BF.7 isolate from Greece, standard enthalpy of formation is -75.41 kJ/C-mol, standard molar entropy is 32.49 J/C-mol K, and

Table 2
Biosynthesis reactions for the nucleocapsids of the BA.5.2 and BF.7 variants of SARS-CoV-2. The general biosynthesis reaction has the form: (Amino acids) + O_2 + HPO_4^{2-} + HCO_3^- → (Bio) + SO_4^{2-} + H_2O + H_2CO_3, where (Bio) denotes the empirical formula of live matter from Table 1. The stoichiometric coefficients for the biosynthesis reactions are given in this table.

Variant	Reactants				→	Products			
	Amino acid	O_2	HPO_4^{2-}	HCO_3^-		Bio	SO_4^{2-}	H_2O	H_2CO_3
BA.5.2 nucleocapsid - Australia	1.3898	0.4908	0.0060	0.0438	→	1	0.0279	0.0536	0.4337
BA.5.2 nucleocapsid - Japan	1.3901	0.4912	0.0060	0.0437	→	1	0.0279	0.0538	0.4338
BA.5.2 nucleocapsid - USA	1.3900	0.4912	0.0060	0.0437	→	1	0.0279	0.0538	0.4338
BF.7 nucleocapsid - China	1.3901	0.4913	0.0060	0.0437	→	1	0.0279	0.0538	0.4338
BF.7 nucleocapsid - Greece	1.3901	0.4913	0.0060	0.0437	→	1	0.0279	0.0538	0.4338
BF.7 nucleocapsid - Serbia	1.3901	0.4913	0.0060	0.0437	→	1	0.0279	0.0538	0.4338

Table 3
Standard thermodynamic properties of live matter of nucleocapsids of the BA.5.2 and BF.7 variants of SARS-CoV-2. This table gives data on standard enthalpies of formation, $\Delta_f H°$, standard molar entropies, $S°_m$, and standard Gibbs energies of formation, $\Delta_f G°$.

Variant	$\Delta_f H°$ (kJ/C-mol)			$S°_m$ (J/C-mol K)			$\Delta_f G°$ (kJ/C-mol)		
BA.5.2 nucleocapsid - Australia	-75.32	±	29.42	32.49	±	6.40	-33.21	±	31.33
BA.5.2 nucleocapsid - Japan	-75.39	±	29.42	32.49	±	6.40	-33.27	±	31.33
BA.5.2 nucleocapsid - USA	-75.39	±	29.42	32.49	±	6.40	-33.27	±	31.33
BF.7 nucleocapsid - China	-75.40	±	29.42	32.49	±	6.40	-33.28	±	31.33
BF.7 nucleocapsid - Greece	-75.41	±	29.42	32.49	±	6.40	-33.29	±	31.33
BF.7 nucleocapsid - Serbia	-75.40	±	29.42	32.49	±	6.40	-33.28	±	31.33

Table 4
Standard thermodynamic properties of biosynthesis of nucleocapsids of the BA.5.2 and BF.7 variants of SARS-CoV-2. This table gives data on standard enthalpies of biosynthesis, $\Delta_{bs} H°$, standard entropies of biosynthesis, $\Delta_{bs} S°$, and standard Gibbs energies of biosynthesis, $\Delta_{bs} G°$.

Variant	$\Delta_{bs}H°$ (kJ/C-mol)			$\Delta_{bs}S°$ (J/C-mol K)			$\Delta_{bs}G°$ (kJ/C-mol)		
BA.5.2 nucleocapsid - Australia	-232.14	±	41.72	-37.29	±	9.62	-221.06	±	44.59
BA.5.2 nucleocapsid - Japan	-232.32	±	41.72	-37.34	±	9.62	-221.23	±	44.59
BA.5.2 nucleocapsid - USA	-232.31	±	41.72	-37.34	±	9.62	-221.22	±	44.59
BF.7 nucleocapsid - China	-232.33	±	41.72	-37.34	±	9.62	-221.24	±	44.58
BF.7 nucleocapsid - Greece	-232.35	±	41.72	-37.35	±	9.62	-221.25	±	44.58
BF.7 nucleocapsid - Serbia	-232.33	±	41.72	-37.34	±	9.62	-221.24	±	44.58

standard Gibbs energy of formation is -33.29 kJ/C-mol. For the nucleocapsid of the BF.7 isolate from Serbia, standard enthalpy of formation is -75.40 kJ/C-mol, standard molar entropy is 32.49 J/C-mol K, and standard Gibbs energy of formation is -33.28 kJ/C-mol.

Table 4 gives standard thermodynamic properties of biosynthesis of nucleocapsids of the BA.5.2 and BF.7 variants of SARS-CoV-2. These include standard enthalpy of biosynthesis, $\Delta_{bs}H°$, standard entropy of biosynthesis, $\Delta_{bs}S°$, and standard Gibbs energy of biosynthesis, $\Delta_{bs}G°$. For the nucleocapsid of the BA.5.2 isolate from Australia, standard enthalpy of biosynthesis is -232.14 kJ/C-mol, standard entropy of biosynthesis is -37.29 J/C-mol K, and standard Gibbs energy of biosynthesis is -221.06 kJ/C-mol. For the nucleocapsid of the BA.5.2 isolate from Japan, standard enthalpy of biosynthesis is -232.32 kJ/C-mol, standard entropy of biosynthesis is -37.34 J/C-mol K, and standard Gibbs energy of biosynthesis is -221.23 kJ/C-mol. For the nucleocapsid of the BA.5.2 isolate from USA, standard enthalpy of biosynthesis is -232.31 kJ/C-mol, standard entropy of biosynthesis is -37.34 J/C-mol K, and standard Gibbs energy of biosynthesis is -221.22 kJ/C-mol. For the nucleocapsid of the BF.7 isolate from China, standard enthalpy of biosynthesis is -232.33 kJ/C-mol, standard entropy of biosynthesis is -37.34 J/C-mol K, and standard Gibbs energy of biosynthesis is -221.24 kJ/C-mol. For the nucleocapsid of the BF.7 isolate from Greece, standard enthalpy of biosynthesis is -232.35 kJ/C-mol, standard entropy of biosynthesis is -37.35 J/C-mol K, and standard Gibbs energy of biosynthesis is -221.25 kJ/C-mol. For the nucleocapsid of the BF.7 isolate from Serbia, standard enthalpy of biosynthesis is -232.33 kJ/C-mol, standard entropy of biosynthesis is -37.34 J/C-mol K, and standard Gibbs energy of biosynthesis is -221.24 kJ/C-mol.

4. Discussion

The story about SARS-CoV-2 is reminiscent of the ancient legend of the Hydra of Lerna, a mythical creature that possessed many heads. Just like the Hydra, SARS-CoV-2 has many poisonous heads (variants). Every time humanity cuts off one head, one variant that has caused a pandemic wave, in its place appears a new one. Unfortunately, Heracles has not yet appeared on the scene. Thus, we need a modern Heracles in form of a vaccine. Starting from 2019, several dozen variants of SARS-CoV-2 appeared, some of which have caused pandemic waves. Globally, as of 5:09pm CET, 4 January 2023, there have been 655,689,115 confirmed cases of COVID-19, including 6,671,624 deaths, reported to WHO 2022. These data make SARS-CoV-2 a modern equivalent of the Hydra of Lerna and Medusa Gorgo, the ancient monsters.

The research on SARS-CoV-2 was started in 2020, with a chemical and thermodynamic characterization of the Hu-1 variant (wild type) [Popovic and Minceva, 2020b]. SARS-CoV-2 has since then mutated several dozen times. In that way, several dozen major variants of SARS-CoV-2 virus appeared, some of which caused pandemic waves. Chemical and thermodynamic characterization of more important known variants of SARS-CoV-2 has been made in the literature [Popovic and Popovic, 2022; Özilgen and Yilmaz, 2021; Yilmaz et al., 2020; Nadi and Özilgen, 2021; Şimşek et al., 2021; Degueldre, 2021; Popovic, 2022a, 2022b, 2022c, 2022d, 2022e, 2022f, 2022g, 2022h, 2022i, 2022j; Gale, 2022; Lucia, 2021, 2020a, 2020b; Kaniadakis et al., 2020; Popovic and Minceva, 2021a, 2020b]. Thus, obviously, great efforts have been made by researchers in the field of biothermodynamics to reveal the thermodynamic background of SARS-CoV-2 particles, their life cycle, as well as interactions performed with various host tissues and other viruses.

Virus-host interactions occur at the host cell membrane and in its cytoplasm [Popovic, 2022b, 2022i]. Both interactions represent chemical processes. The interaction at the membrane is similar to protein-ligand interactions [Popovic and Popovic, 2022; Du et al., 2016]. The interaction in the cytoplasm represents a polymerization reaction of nucleotides and amino acids into nucleic acids and proteins, respectively [Pinheiro et al., 2008; Lee et al., 2020; Dodd et al., 2020; Johansson and Dixon, 2013]. These reactions are competitive. The competition is performed between the virus and its host cell. The driving force for the antigen-receptor binding at the membrane and the polymerization of nucleotides into nucleic acids and synthesis of proteins is Gibbs energy [von Stockar, 2013a, 2013b; von Stockar and Liu, 1999; Demirel, 2014, Balmer, 2010; Berg et al., 2002]. Mutations of SARS-CoV-2 that appeared during time have led to change in empirical formula of new variants [Popovic, 2022i]. Changes in empirical formula have led to change in thermodynamic properties of binding and biosynthesis [Popovic, 2022f, 2022g, 2022i]. Changes in thermodynamic properties caused changes in kinetic parameters, including antigen-receptor binding rate and rate of biosynthesis of viral components, according to the phenomenological equations [Popovic, 2022f, 2022g, 2022i]. Changes in the kinetics have led to changes in infectivity and pathogenicity [Popovic, 2022e, 2022i].

Every time a new variant appears, a question is raised about its infectivity and pathogenicity. Thus, with appearance of new BA.5.2 and BF.7 variants, the question was raised of whether they will be able to cause a new pandemic wave. The new variants compete with the old variants, if they appear at the same time in the same place. In that

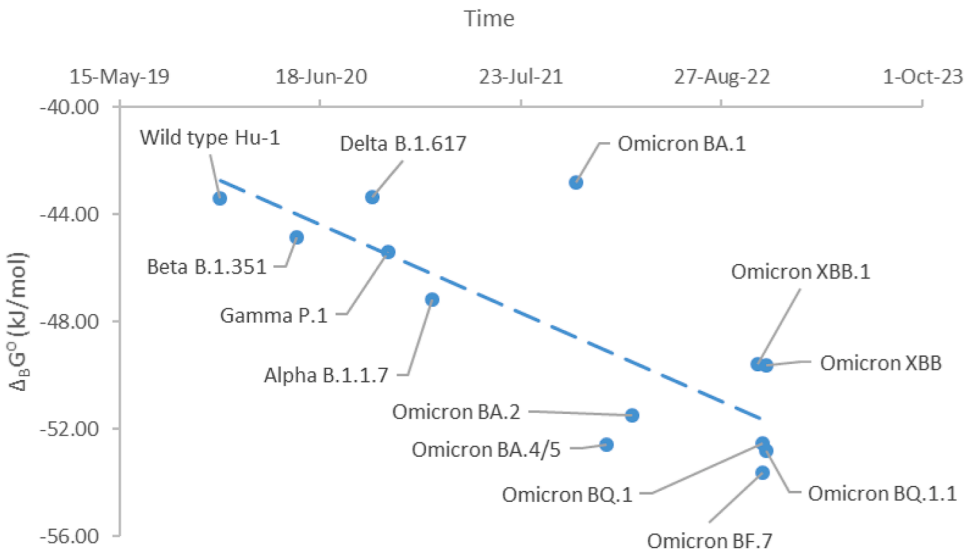

Fig. 1. Gibbs energies of binding through evolution of SARS-CoV-2. This graph shows standard Gibbs energies of binding, $\Delta_B G^o$, of SARS-CoV-2 variants during their evolution. The graph starts from the Hu-1 variant (Wild type) that appeared in late 2019 and ends with the newest BF.7 variant. The blue dots represent Gibbs energies of binding of the SARS-CoV-2 variants. The blue dashed line represents the direction of evolution of the $\Delta_B G^o$ values.

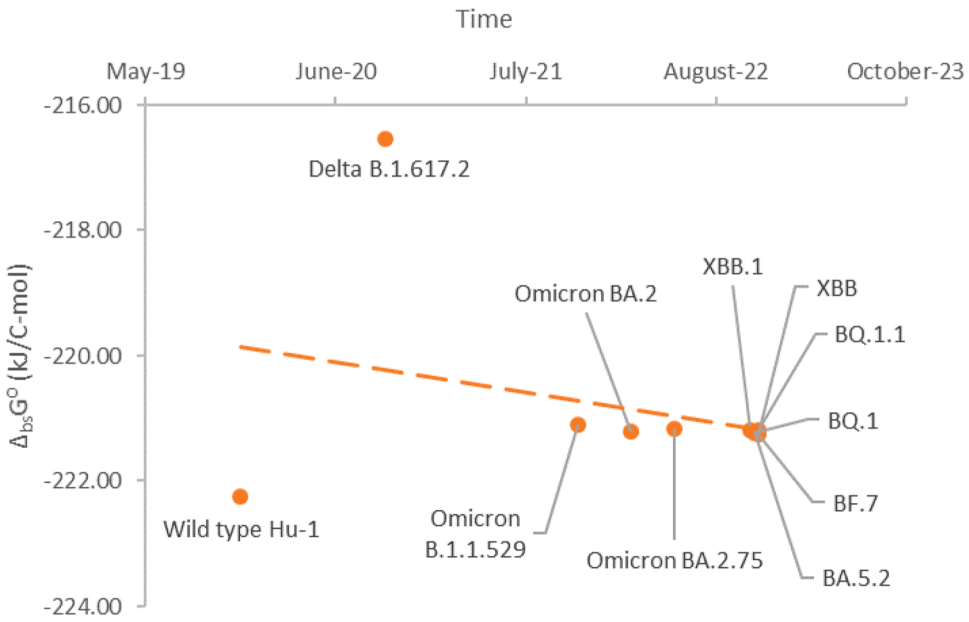

Fig. 2. Gibbs energy of biosynthesis through evolution of SARS-CoV-2. This graph shows standard Gibbs energies of biosynthesis, $\Delta_{bs} G^o$, of SARS-CoV-2 variants during their evolution. The graph starts from the Hu-1 variant (Wild type) that appeared in late 2019 and ends with the newest BA.5.2 and BF.7 variants. The orange dots represent Gibbs energies of binding of the SARS-CoV-2 variants. The orange dashed line represents the direction of evolution of the $\Delta_{bs} G^o$ values.

competition, one variant will win and suppress and weaker one. To predict the outcome of the competition, it is necessary to know the Gibbs energy of binding and Gibbs energy of biosynthesis. In this paper, for the first time, standard Gibbs energy of binding was determined for the BF.7 variant. It is -53.64 kJ/C-mol, at 25°C. Fig. 1 shows Gibbs energies of binding of various variants of SARS-CoV-2. From Fig. 1, it is possible to see the trend of evolution of SARS-CoV-2 towards more negative Gibbs energy of binding. More negative Gibbs energy of binding leads to greater antigen-receptor binding rate, which in turn leads to increased infectivity [Popovic, 2022g].

Fig. 2 shows Gibbs energies of biosynthesis through evolution of SARS-CoV-2 variants from Hu-1 to Omicron BA.5.2 and BF.7. All the Omicron variants are characterized by very similar Gibbs energies of biosynthesis. Gibbs energies of biosynthesis of all Omicron variants are slightly less negative than that of the Hu-1 variant. According to the phenomenological equations, this indicates a slightly slower multiplication of new variants compared to Hu-1. The slower multiplication leads to lesser range of damage to host tissues. This coincides with the fact that the number of more severe cases in any of the Omicron variants is lower than that of Hu-1. From this we can conclude that during evolution, mutations in the part of the SARS-CoV-2 genome that encodes proteins other than the spike glycoprotein have led to a decrease in pathogenicity. Indeed, from the evolutionary perspective, the favored mutations are those that lead to increase in infectivity and maintenance or slight decrease in pathogenicity [Popovic, 2022e]. Thus, in the wave that is currently hitting China and is dominated by the BF.7 variant, it is possible to expect an increased number of newly infected cases, due to an increase in infectivity, but without an increase in the number of

severe cases, having in mind that pathogenicity has not significantly changed compared to the earlier variants. However, it is obvious that due to the significant difference in Gibbs energy of binding, BF.7 should be able to suppress other Omicron variants that are in circulation.

5. Conclusions

Gibbs energy of antigen-receptor binding of Omicron BF.7 is more negative than that of the other variants. Thus, the rate of antigen-receptor binding of Omicron BF.7 is greater than that of other variants present in the population. This leads to an increased infectivity of BF.7 and probable domination in the next wave of the COVID-19 pandemic.

Gibbs energy of biosynthesis of BA.5.2 and BF.7 is not significantly different than the Gibbs energy of biosynthesis of other Omicron variants. The rate of biosynthesis of BF.7 and BA.5.2 is approximately equal to the biosynthesis rate of other Omicron variants. The pathogenicity of BF.7 and BA.5.2 variants should not be greater than those of other Omicron variants.

CRediT authorship contribution statement

Marko Popovic: Conceptualization, Methodology, Software, Validation, Formal analysis, Investigation, Writing – original draft, Writing – review & editing, Visualization.

Declaration of Competing Interest

The author declares no conflict of interest.

Acknowledgments

The author gratefully acknowledges all data contributors, i.e., the Authors and their Originating laboratories responsible for obtaining the specimens, and their Submitting laboratories for generating the genetic sequence and metadata and sharing via the GISAID Initiative, on which this research is based.

Supplementary materials

Supplementary material associated with this article can be found, in the online version, at doi:10.1016/j.mran.2023.100249.

References

Aladag, A., Hoffmann, S., Stoldt, M., Bösing, C., Willbold, D., Schwarten, M., 2014. Hepatitis C virus NS5A is able to competitively displace c-Myc from the Bin1 SH3 domain in vitro. J. Peptide Sci.: Off. Publ. Euro. Peptide Soc. 20 (5), 334–340. https://doi.org/10.1002/psc.2618.

Anasir, M.I., Caria, S., Skinner, M.A., Kvansakul, M., 2017. Structural basis of apoptosis inhibition by the fowlpox virus protein FPV039. J. Biol. Chem. 292 (22), 9010–9021. https://doi.org/10.1074/jbc.M116.768879.

Atkins, P. W., & de Paula, J. (2011). Physical Chemistry for the Life Sciences (2nd edition), W. H. Freeman and Company. ISBN-13: 978-1429231145.

Atkins, P.W., de Paula, J., 2014. Physical Chemistry: Thermodynamics, Structure, and Change, 10thEdition. W. H. Freeman and Company, New York. ISBN-13: 978-1429290197.

Balmer, R.T., 2010. Modern Engineering Thermodynamics. Academic Press, Cambridge, MA. https://doi.org/10.1016/C2009-0-20199-1.

Banerjee, M., Speir, J.A., Kwan, M.H., Huang, R., Aryanpur, P.P., Bothner, B., Johnson, J. E., 2010. Structure and function of a genetically engineered mimic of a nonenveloped virus entry intermediate. J. Virol. 84 (9), 4737–4746. https://doi.org/10.1128/JVI.02670-09.

Battley, E.H., Stone, J.R., 2000. A comparison of values for the entropy and the entropy of formation of selected organic substances of biological importance in the solid state, as determined experimentally or calculated empirically. Thermochim. Acta 349 (1-2), 153–161. https://doi.org/10.1016/S0040-6031(99)00509-2.

Battley, E.H., 1999. An empirical method for estimating the entropy of formation and the absolute entropy of dried microbial biomass for use in studies on the thermodynamics of microbial growth. Thermochim. Acta 326 (1-2), 7–15. https://doi.org/10.1016/S0040-6031(98)00584-X.

Battley, E.H., 1998. The development of direct and indirect methods for the study of the thermodynamics of microbial growth. Thermochim. Acta 309 (1-2), 17–37. https://doi.org/10.1016/S0040-6031(97)00357-2.

Battley, E.H., 1992. On the enthalpy of formation of Escherichia coli K-12 cells. Biotechnol. Bioeng. 39, 5–12. https://doi.org/10.1002/bit.260390103.

Bauer, D.W., Li, D., Huffman, J., Homa, F.L., Wilson, K., Leavitt, J.C., Casjens, S.R., Baines, J., Evilevitch, A., 2015. Exploring the Balance between DNA Pressure and Capsid Stability in Herpesviruses and Phages. J. Virol. 89 (18), 9288–9298. https://doi.org/10.1128/JVI.01172-15.

Bauer, D.W., Huffman, J.B., Homa, F.L., Evilevitch, A., 2013. Herpes virus genome, the pressure is on. J. Am. Chem. Soc. 135 (30), 11216–11221. https://doi.org/10.1021/ja404008r.

Berg, J.M., Tymoczko, J.L., Stryer, L., 2002. Biochemistry, 5th ed. W H Freeman, New York. ISBN-13: 978-0716746843.

Boltzmann, L. (1974). The second law of thermodynamics. In: Theoretical Physics and Philosophical Problems, McGuinnes, B., ed., Boston, MA: D. Riedel Publishing Company, LLC. ISBN 978-90-277-0250-0 (translation of the original version published in 1886).

Britannica (2023). Hydra – Greek mythology [Online] Available at: https://www.britannica.com/topic/Hydra-Greek-mythology (Accessed on February 1, 2023).

Brouillette, C.G., Compans, R.W., Brandts, J.F., Segrest, J.P., 1982. Structural domains of vesicular stomatitis virus. A study by differential scanning calorimetry, thermal gel analysis, and thermal electron microscopy. J. Biol. Chem. 257 (1), 12–15. PMID: 6273421.

Byrn, R.A., Jones, S.M., Bennett, H.B., Bral, C., Clark, M.P., Jacobs, M.D., Kwong, A.D., Ledeboer, M.W., Leeman, J.R., McNeil, C.F., Murcko, M.A., Nezami, A., Perola, E., Rijnbrand, R., Saxena, K., Tsai, A.W., Zhou, Y., Charifson, P.S., 2015. Preclinical activity of VX-787, a first-in-class, orally bioavailable inhibitor of the influenza virus polymerase PB2 subunit. Antimicrob. Agents Chemother. 59 (3), 1569–1582. https://doi.org/10.1128/AAC.04623-14.

Degueldre, C., 2021. Single virus inductively coupled plasma mass spectroscopy analysis: a comprehensive study. Talanta 228, 122211. https://doi.org/10.1016/j.talanta.2021.122211.

Demirel, Y., 2014. Nonequilibrium Thermodynamics: Transport and Rate Processes in Physical, Chemical and Biological Systems, 3rded, ISBN. Elsevier, Amsterdam, 9780444595812.

Deschuyteneer, M., Elouahabi, A., Plainchamp, D., Plisnier, M., Soete, D., Corazza, Y., Lockman, L., Giannini, S., Deschamps, M., 2010. Molecular and structural characterization of the L1 virus-like particles that are used as vaccine antigens in Cervarix™, the AS04-adjuvanted HPV-16 and -18 cervical cancer vaccine. Hum. Vacc. 6 (5), 407–419. https://doi.org/10.4161/hv.6.5.11023.

Djamali, E., Nulton, J.D., Turner, P.J., Rohwer, F., Salamon, P., 2012. Heat output by marine microbial and viral communities. J. NonEquilib. Thermodyn. 37 (3), 291–313. https://doi.org/10.1515/jnetdy-2011-0235.

Dodd, T., Botto, M., Paul, F., et al., 2020. Polymerization and editing modes of a high-fidelity DNA polymerase are linked by a well-defined path. Nat. Commun. 11, 5379. https://doi.org/10.1038/s41467-020-19165-2.

Du, X., Li, Y., Xia, Y.L., Ai, S.M., Liang, J., Sang, P., Liu, S.Q., 2016. Insights into protein–ligand interactions: mechanisms, models, and methods. Int. J. Mol. Sci. 17 (2), 144. https://doi.org/10.3390/ijms17020144.

Duan, L., Zheng, Q., Zhang, H., Niu, Y., Lou, Y., Wang, H., 2020. The SARS-CoV-2 spike glycoprotein biosynthesis, structure, function, and antigenicity: implications for the design of spike-based vaccine immunogens. Front. Immunol. 11, 576622 https://doi.org/10.3389/fimmu.2020.576622.

Elbe, S., Buckland-Merrett, G., 2017. Data, disease and diplomacy: GISAID's innovative contribution to global health. Glob. Challenges 1, 33–46. https://doi.org/10.1002/gch2.1018. PMCID: 31565258.

Euripides (2023). Heracles: 1270-1280 [Online] Perseus Digital Library. Available at: http://data.perseus.org/citations/urn:cts:greekLit:tlg0006.tlg009.perseus-eng1:1255-1293 (Accessed on February 1, 2023) (English translation of the original tragedy "Ἡρακλῆς μαινόμενος" written in Greek around 416 BC).

Fanaei Pirlar, R., Wagemans, J., Ponce Benavente, L., Lavigne, R., Trampuz, A., Gonzalez Moreno, M., 2022. Novel bacteriophage specific against staphylococcus epidermidis and with antibiofilm activity. Viruses 14 (6), 1340. https://doi.org/10.3390/v14061340. MDPI AG. Retrieved from.

Gale, P., 2022. Using thermodynamic equilibrium models to predict the effect of antiviral agents on infectivity: Theoretical application to SARS-CoV-2 and other viruses. Microb. Risk Anal. 21, 100198 https://doi.org/10.1016/j.mran.2021.100198.

Gao, X., Zhu, K., Qin, B., Olieric, V., Wang, M., Cui, S., 2021. Crystal structure of SARS-CoV-2 Orf9b in complex with human TOM70 suggests unusual virus-host interactions. Nat. Commun. 12 (1), 2843. https://doi.org/10.1038/s41467-021-23118-8.

Gelman, D., Yerushalmy, O., Alkalay-Oren, S., Rakov, C., Ben-Porat, S., Khalifa, L., Adler, K., Abdalrhman, M., Coppenhagen-Glazer, S., Aslam, S., Schooley, R.T., Nir-Paz, R., Hazan, R., 2021. Clinical phage microbiology: a suggested framework and recommendations for the in-vitro matching steps of phage therapy. Lancet. Microbe 2 (10), e555–e563. https://doi.org/10.1016/S2666-5247(21)00127-0.

Glansdorff, P., Prigogine, I., 1971. Thermodynamic Theory of Structure, Stability and Fluctuations. Wiley, Hoboken, NJ, pp. 978–0471302803. ISBN-13.

Guosheng, L., Yi, L., Xiangdong, C., Peng, L., Ping, S., Songsheng, Q., 2003. Study on interaction between T4 phage and Escherichia coli B by microcalorimetric method. J. Virol. Methods 112 (1-2), 137–143. https://doi.org/10.1016/s0166-0934(03)00214-3.

Hesiod (2023). Theogony: 310-320 [Online] Perseus Digital Library. Available at: http://data.perseus.org/citations/urn:cts:greekLit:tlg0020.tlg001.perseus-eng1:304-336

(Accessed on February 1, 2023) (English translation of the original poem "Θεογονία" written in Greek around 730-700 BC).
Istifli, E.S., Netz, P.A., Sihoglu Tepe, A., Sarikurkcu, C., Tepe, B., 2022. Understanding the molecular interaction of SARS-CoV-2 spike mutants with ACE2 (angiotensin converting enzyme 2). J. Biomol. Struct. Dyn. 40 (23), 12760–12771. https://doi.org/10.1080/07391102.2021.1975569.
Javorsky, A., Maddumage, J. C., Mackie, E., Soares da Costa, T. P., Humbert, P. O., & Kvansakul, M. (2022). Structural insight into the Scribble PDZ domains interaction with the oncogenic Human T-cell lymphotrophic virus-1 (HTLV-1) Tax1 PBM. *The FEBS journal*, 10.1111/febs.16607. Advance online publication. https://doi.org/10.1111/febs.16607.
Johansson, E., & Dixon, N. (2013). Replicative DNA polymerases. *Cold Spring Harbor perspectives in biology*, 5(6), a012799. https://doi.org/10.1101/cshperspect.a012799.
Kaniadakis, G., Baldi, M.M., Deisboeck, T.S., Grisolia, G., Hristopulos, D.T., Scarfone, A. M., Sparavigna, A., Wada, T., Lucia, U., 2020. The κ-statistics approach to epidemiology. Sci. Rep. 10 (1), 19949. https://doi.org/10.1038/s41598-020-76673-3.
Katen, S., Zlotnick, A., 2009. The thermodynamics of virus capsid assembly. Methods Enzymol. 455, 395–417. https://doi.org/10.1016/S0076-6879(08)04214-6.
Kawahara, T., Akiba, I., Sakou, M., Sakaguchi, T., Taniguchi, H., 2018. Inactivation of human and avian influenza viruses by potassium oleate of natural soap component through exothermic interaction. PLoS One 13 (9), e0204908. https://doi.org/10.1371/journal.pone.0204908.
Khare, S., et al., 2021. GISAID's role in pandemic response. China CDC Wkly. 3 (49), 1049–1051. https://doi.org/10.46234/ccdcw2021.255. PMCID: 8668406.
Krell, T., Manin, C., Nicolaï, M.C., Pierre-Justin, C., Bérard, Y., Brass, O., Gérentes, L., Leung-Tack, P., Chevalier, M., 2005. Characterization of different strains of poliovirus and influenza virus by differential scanning calorimetry. Biotechnol. Appl. Biochem. 41, 241–246. https://doi.org/10.1042/BA20040113. Pt 3.
Lee, J., Schwarz, K.J., Kim, D.S., Moore, J.S., Jewett, M.C., 2020. Ribosome-mediated polymerization of long chain carbon and cyclic amino acids into peptides in vitro. Nat. Commun. 11 (1), 4304. https://doi.org/10.1038/s41467-020-18001-x.
Liu, T., Sae-Ueng, U., Li, D., Lander, G.C., Zuo, X., Jönsson, B., Rau, D., Shefer, I., Evilevitch, A., 2014. Solid-to-fluid-like DNA transition in viruses facilitates infection. Proc. Nat. Acad. Sci. U.S.A. 111 (41), 14675–14680. https://doi.org/10.1073/pnas.1321637111.
Lucia, U., Grisolia, G., Deisboeck, T.S., 2021. Thermodynamics and SARS-CoV-2: neurological effects in post-Covid 19 syndrome. Atti Della Accad. Pelorit. Pericol. 99 (2), A3. https://doi.org/10.1478/AAPP.992A3.
Lucia, U., Grisolia, G., Deisboeck, T.S., 2020a. Seebeck-like effect in SARS-CoV-2 bio-thermodynamics. Atti Della Accad. Pelorit. Pericol. -Classe Sci. Fisich., Matem. Nat. 98 (2), 6. https://doi.org/10.1478/AAPP.982A6.
Lucia, U., Deisboeck, T.S., Grisolia, G., 2020b. Entropy-based pandemics forecasting. Front. Phys. 8, 274. https://doi.org/10.3389/fphy.2020.00274.
Maassen, S.J., Huskens, J., Cornelissen, J.J.L.M., 2019. Elucidating the thermodynamic driving forces of polyanion-templated virus-like particle assembly. J. Phys. Chem. B 123 (46), 9733–9741. https://doi.org/10.1021/acs.jpcb.9b06258.
Makarov, V.V., Skurat, E.V., Semenyuk, P.I., Abashkin, D.A., Kalinina, N.O., Arutyunyan, A.M., Solovyev, A.G., Dobrov, E.N., 2013. Structural lability of Barley stripe mosaic virus virions. PLoS One 8 (4), e60942. https://doi.org/10.1371/journal.pone.0060942.
Maskow, T., Kiesel, B., Schubert, T., Yong, Z., Harms, H., Yao, J., 2010. Calorimetric real time monitoring of lambda prophage induction. J. Virol. Methods 168 (1-2), 126–132. https://doi.org/10.1016/j.jviromet.2010.05.002.
Molla, A., Paul, A.V., Wimmer, E., 1991. Cell-free, de novo synthesis of poliovirus. Science (New York, N.Y.) 254 (5038), 1647–1651. https://doi.org/10.1126/science.1661029.
Morais, F.M., Buchholz, F., Hartmann, T., et al., 2014. Chip-calorimetric monitoring of biofilm eradication with bacteriophages reveals an unexpected infection-related heat profile. J. Therm. Anal. Calorim. 115, 2203–2210. https://doi.org/10.1007/s10973-013-3494-4.
Morowitz, H.J., Kostelnik, J.D., Yang, J., Cody, G.D., 2000. The origin of intermediary metabolism. Proc. Natl Acad. Sci. 97 (14), 7704–7708. https://doi.org/10.1073/pnas.110153997.
Morowitz, H., 1995. The emergence of complexity. Complex. 1 (1), 4–5. https://doi.org/10.1002/cplx.6130010102.
Morowitz, H.J., 1992. Beginnings of Cellular Life: Metabolism Recapitulates Biogenesis. Yale University Press, New Haven, CT.
Morowitz, H.J., Heinz, B., Deamer, D.W., 1988. The chemical logic of a minimum protocell. Origins Life Evol. Biosphere 18, 281–287. https://doi.org/10.1007/BF01804674.
Morowitz, H.J., 1976. The high cost of being human. The New York Times 11, 45. FebruaryAvailable at. https://www.nytimes.com/1976/02/11/archives/the-high-cost-of-being-human.html.
Morowitz, H.J., 1968. Energy Flow in Biology: Biological Organization as a Problem in Thermal Physics. Academic Press, New York.
Morowitz, H.J., 1955. Some order-disorder considerations in living systems. Bull. Math. Biophys. 17, 81–86. https://doi.org/10.1007/BF02477985.
Nadi, F., Özilgen, M., 2021. Effects of COVID-19 on energy savings and emission reduction: a case study. Int. J. Glob. Warm. 25 (1), 38–57. https://doi.org/10.1504/IJGW.2021.117432.
National Center for Biotechnology Information (2022). NCBI Database [online]. Available at: https://www.ncbi.nlm.nih.gov/ (Accessed on January 7, 2023)..
Nebel, S., Bartoldus, I., Stegmann, T., 1995. Calorimetric detection of influenza virus induced membrane fusion. Biochemistry 34 (17), 5705–5711. https://doi.org/10.1021/bi00017a001.
Noble, C.G., Lim, S.P., Arora, R., Yokokawa, F., Nilar, S., Seh, C.C., Wright, S.K., Benson, T.E., Smith, P.W., Shi, P.Y., 2016. A conserved pocket in the dengue virus polymerase identified through fragment-based screening. J. Biol. Chem. 291 (16), 8541–8548. https://doi.org/10.1074/jbc.M115.710731.
Neuman, B.W., Buchmeier, M.J., 2016. Supramolecular architecture of the coronavirus particle. Adv. Virus Res. 96, 1–27. https://doi.org/10.1016/bs.aivir.2016.08.005.
Neuman, B.W., Kiss, G., Kunding, A.H., Bhella, D., Baksh, M.F., Connelly, S., Droese, B., Klaus, J.P., Makino, S., Sawicki, S.G., Siddell, S.G., Stamou, D.G., Wilson, I.A., Kuhn, P., Buchmeier, M.J., 2011. A structural analysis of M protein in coronavirus assembly and morphology. J. Struct. Biol. 174 (1), 11–22. https://doi.org/10.1016/j.jsb.2010.11.021.
Neuman, B.W., Adair, B.D., Yoshioka, C., Quispe, J.D., Orca, G., Kuhn, P., Milligan, R.A., Yeager, M., Buchmeier, M.J., 2006. Supramolecular architecture of severe acute respiratory syndrome coronavirus revealed by electron cryomicroscopy. J. Virol. 80 (16), 7918–7928. https://doi.org/10.1128/JVI.00645-06.
Ozilgen, M., Sorgüven, E., 2017. Biothermodynamics: Principles and Applications. CRC Press, Boca Raton. https://doi.org/10.1201/9781315374147.
Özilgen, M., Yilmaz, B., 2021. COVID-19 disease causes an energy supply deficit in a patient. Int. J. Energy Res. 45 (2), 1157–1160. https://doi.org/10.1002/er.5883.
Patel, S.A., Erickson, L.E., 1981. Estimation of heats of combustion of biomass from elemental analysis using available electron concepts. Biotechnol. Bioeng. 23, 2051–2067. https://doi.org/10.1002/bit.260230910.
Pinheiro, A.V., Baptista, P., Lima, J.C., 2008. Light activation of transcription: photocaging of nucleotides for control over RNA polymerization. Nucleic. Acids. Res. 36 (14), e90. https://doi.org/10.1093/nar/gkn415.
Popovic, M. (2023). Simple but powerful: viroids can hijack their host cells' metabolism due to greater Gibbs energy dissipation. Preprints, 2023010085. https://doi.org/10.20944/preprints202301.0085.v1.
Popovic, M., & Popovic, M. (2022). Strain Wars: Competitive interactions between SARS-CoV-2 strains are explained by Gibbs energy of antigen-receptor binding. *Microb. Risk Anal.*, 21, 100202. https://doi.org/10.1016/j.mran.2022.100202.
Popovic, M., 2022a. Strain wars 2: Binding constants, enthalpies, entropies, Gibbs energies and rates of binding of SARS-CoV-2 variants. Virology 570, 35–44. https://doi.org/10.1016/j.virol.2022.03.008.
Popovic, M., 2022b. Strain wars 3: Differences in infectivity and pathogenicity between Delta and Omicron strains of SARS-CoV-2 can be explained by thermodynamic and kinetic parameters of binding and growth. Microb. Risk Anal. 22, 100217 https://doi.org/10.1016/j.mran.2022.100217.
Popovic, M., 2022c. Strain wars 4 - Darwinian evolution through Gibbs' glasses: Gibbs energies of binding and growth explain evolution of SARS-CoV-2 from Hu-1 to BA.2. Virology 575, 36–42. https://doi.org/10.1016/j.virol.2022.08.009.
Popovic, M., 2022d. Strain wars 5: Gibbs energies of binding of BA.1 through BA.4 variants of SARS-CoV-2. Microb. Risk Anal. 22, 100231 https://doi.org/10.1016/j.mran.2022.100231.
Popovic, M., 2022e. Beyond COVID-19: Do biothermodynamic properties allow predicting the future evolution of SARS-CoV-2 variants? Microb. Risk Anal. 22, 100232 https://doi.org/10.1016/j.mran.2022.100232.
Popovic, M., 2022f. Omicron BA.2.75 sublineage (centaurus) follows the expectations of the evolution theory: less negative gibbs energy of biosynthesis indicates decreased pathogenicity. Microbiol. Res. 13 (4), 937–952. https://doi.org/10.3390/microbiolres13040066. MDPI AG. Retrieved from.
Popovic, M., 2022g. Omicron BA.2.75 subvariant of SARS-CoV-2 is expected to have the greatest infectivity compared with the competing BA.2 and BA.5, due to most negative Gibbs energy of binding. BioTech 11 (4), 45. https://doi.org/10.3390/biotech11040045. MDPI AG. Retrieved from.
Popovic, M., 2022h. Never ending story? Biothermodynamic properties of biosynthesis and binding of omicron BQ.1, BQ.1.1, XBB and XBB.1 variants of SARS-CoV-2. Preprints, 2022120122. https://doi.org/10.20944/preprints202212.0122.v1.
Popovic, M., 2022i. Biothermodynamics of viruses from absolute zero (1950) to virothermodynamics, 2022 Vaccines 10 (12). https://doi.org/10.3390/vaccines10122112, 2112.
Popovic, M., 2022j. Why doesn't Ebola virus cause pandemics like SARS-CoV-2? Microb. Risk Anal. 22, 100236 https://doi.org/10.1016/j.mran.2022.100236.
Popovic, M., 2022k. Atom counting method for determining elemental composition of viruses and its applications in biothermodynamics and environmental science. Comput. Biol. Chem. 96, 107621 https://doi.org/10.1016/j.compbiolchem.2022.107621.
Popovic, M., 2022L. Formulas for death and life: Chemical composition and biothermodynamic properties of Monkeypox (MPV, MPXV, HMPXV) and Vaccinia (VACV) viruses. Therm. Sci. 26 (6A) https://doi.org/10.2298/TSCI220524142P.
Popovic, M., 2022m. Everything you always wanted to know about the biothermodynamic background of herpes simplex virus type 1 – host interaction. Preprints, 2022120063. https://doi.org/10.20944/preprints202212.0063.v1.
Popovic, M., 2022n. Standard Gibbs energy of binding of the gp120 antigen of HIV-1 to the CD4 receptor. Preprints, 2022110482. https://doi.org/10.20944/preprints202211.0482.v1.
Popovic, M., 2022p. Biothermodynamic key opens the door of life sciences: bridging the gap between biology and thermodynamics. Preprints, 2022100326. https://doi.org/10.20944/preprints202210.0326.v1.
Popovic, M., 2022q. Thermodynamics of bacteria-phage interactions: T4 and lambda bacteriophages, and E. Coli can coexist in natural ecosystems due to the ratio of their gibbs energies of biosynthesis. Preprints, 2022110327. https://doi.org/10.20944/preprints202211.0327.v1.

Popovic, M., Minceva, M., 2021a. Coinfection and Interference Phenomena Are the Results of Multiple Thermodynamic Competitive Interactions. Microorganisms 9 (10), 2060. https://doi.org/10.3390/microorganisms9102060.
Popovic, M., Minceva, M., 2020a. A thermodynamic insight into viral infections: do viruses in a lytic cycle hijack cell metabolism due to their low Gibbs energy? Heliyon 6 (5), e03933. https://doi.org/10.1016/j.heliyon.2020.e03933.
Popovic, M., & Minceva, M. (2020b). Thermodynamic insight into viral infections 2: empirical formulas, molecular compositions and thermodynamic properties of SARS, MERS and SARS-CoV-2 (COVID-19) viruses. *Heliyon*, 6(9), e04943. https://doi.org/10.1016.2Fj.heliyon.2020.e04943.
Popovic, M., 2019. Thermodynamic properties of microorganisms: determination and analysis of enthalpy, entropy, and Gibbs free energy of biomass, cells and colonies of 32 microorganism species. Heliyon 5 (6), e01950. https://doi.org/10.1016/j.heliyon.2019.e01950.
Popovic, M., 2018a. Living organisms from Prigogine's perspective: an opportunity to introduce students to biological entropy balance. J. Biol. Educ. 52 (3), 294–300. https://doi.org/10.1080/00219266.2017.1357649.
Popovic, M., 2018b. Research in entropy wonterland: a review of the entropy concept. Therm. Sci. 22 (2), 1163–1178. https://doi.org/10.2298/TSCI180115012P.
Prins, K.C., Binning, J.M., Shabman, R.S., Leung, D.W., Amarasinghe, G.K., Basler, C.F., 2010. Basic residues within the ebolavirus VP35 protein are required for its viral polymerase cofactor function. J. Virol. 84 (20), 10581–10591. https://doi.org/10.1128/JVI.00925-10.
Prigogine, I., Wiame, J.M., 1946. Biologie et thermodynamique des phénomènes irréversibles. Experientia 2, 451–453. https://doi.org/10.1007/BF02153597.
Prigogine, I. (1977). Nobel lecture: time, structure and fluctuations. [Online] Available at: https://www.nobelprize.org/prizes/chemistry/1977/prigogine/lecture/ (Accessed on: January 5, 2023).
Prigogine, I., 1947. Etude Thermodynamique des Phénomènes Irréversibles. Dunod. WorldCat ID, Paris, 421502786.
Privalov, P.L., 2012. Microcalorimetry of Macromolecules: the Physical Basis of Biological Structures. John Wiley & Sons, Hoboken, NJ. ISBN978-1-118-10451-4.
Ridgway, H., Chasapis, C.T., Kelaidonis, K., Ligielli, I., Moore, G.J., Gadanec, L.K., Zulli, A., Apostolopoulos, V., Mavromoustakos, T., Matsoukas, J.M., 2022. Understanding the driving forces that trigger mutations in SARS-CoV-2: mutational energetics and the role of arginine blockers in COVID-19 therapy. Viruses 14, 1029. https://doi.org/10.3390/v14051029.
Sarge, S.M., Höhne, G.W., Hemminger, W., 2014. Calorimetry: Fundamentals, Instrumentation and Applications. John Wiley & Sons, Hoboken, NJ. ISBN: 978-3-527-32761-4.
Sayers, E.W., Bolton, E.E., Brister, J.R., Canese, K., Chan, J., Comeau, D.C., Connor, R., Funk, K., Kelly, C., Kim, S., Madej, T., Marchler-Bauer, A., Lanczycki, C., Lathrop, S., Lu, Z., Thibaud-Nissen, F., Murphy, T., Phan, L., Skripchenko, Y., Tse, T., Sherry, S. T., 2022. Database resources of the national center for biotechnology information. Nucleic. Acids. Res. 50 (D1), D20–D26. https://doi.org/10.1093/nar/gkab1112.
Schrödinger, E., 1944. What is Life? The Physical Aspect of the Living Cell. Cambridge university press, Cambridge. ISBN: 0-521-42708-8.
Scialo, F., Daniele, A., Amato, F., Pastore, L., Matera, M.G., Cazzola, M., Castaldo, G., Bianco, A., 2020. ACE2: the major cell entry receptor for SARS-CoV-2. Lung 198 (6), 867–877. https://doi.org/10.1007/s00408-020-00408-4.
Shadrick, W.R., Mukherjee, S., Hanson, A.M., Sweeney, N.L., Frick, D.N., 2013. Aurintricarboxylic acid modulates the affinity of hepatitis C virus NS3 helicase for both nucleic acid and ATP. Biochemistry 52 (36), 6151–6159. https://doi.org/10.1021/bi4006495.
Sigg, A.P., Mariotti, M., Grütter, A.E., Lafranca, T., Leitner, L., Bonkat, G., Braissant, O., 2022. A method to determine the efficacy of a commercial phage preparation against uropathogens in urine and artificial urine determined by isothermal microcalorimetry. *microorganisms*. MDPI AG 10 (5), 845. https://doi.org/10.3390/microorganisms10050845. Retrieved from.
Şimşek, B., Özilgen, M., Utku, F.Ş., 2021. How much energy is stored in SARS-CoV-2 and its structural elements? Energy Storage e298. https://doi.org/10.1002/est2.298.
Sharma, R., Fatma, B., Saha, A., Bajpai, S., Sistla, S., Dash, P.K., Parida, M., Kumar, P., Tomar, S., 2016. Inhibition of chikungunya virus by picolinate that targets viral capsid protein. Virology 498, 265–276. https://doi.org/10.1016/j.virol.2016.08.029.
Shu, Y., McCauley, J., 2017. GISAID: from vision to reality. EuroSurveillance 22 (13). https://doi.org/10.2807/1560-7917.ES.2017.22.13.30494. PMCID: PMC5388101.
Stauffer, H., Srinivasan, S., Lauffer, M.A., 1970. Calorimetric studies on polymerization-depolymerization of tobacco mosaic virus protein. Biochemistry 9 (2), 193–200. https://doi.org/10.1021/bi00804a001.
Sturtevant, J.M., Velicelebi, G., Jaenicke, R., Lauffer, M.A., 1981. Scanning calorimetric investigation of the polymerization of the coat protein of tobacco mosaic virus. Biochemistry 20 (13), 3792–3800. https://doi.org/10.1021/bi00516a019.
Tkhilaishvili, T. (2022). *Bacteriophages as an alternative strategy in the treatment and prevention of implant-associated infections* (Doctoral dissertation). http://doi.org/10.17169/refubium-32604.
Tkhilaishvili, T., Wang, L., Tavanti, A., Trampuz, A., Di Luca, M., 2020a. Antibacterial efficacy of two commercially available bacteriophage formulations, staphylococcal bacteriophage and PYO bacteriophage, against methicillin-resistant *Staphylococcus aureus*: prevention and eradication of biofilm formation and control of a systemic infection of *Galleria mellonella* Larvae. Front. Microbiol. 11, 110. https://doi.org/10.3389/fmicb.2020.00110.
Tkhilaishvili, T., Wang, L., Perka, C., Trampuz, A., Gonzalez Moreno, M., 2020b. Using bacteriophages as a trojan horse to the killing of dual-species biofilm formed by *Pseudomonas aeruginosa* and methicillin resistant *Staphylococcus aureus*. Front. Microbiol. 11, 695. https://doi.org/10.3389/fmicb.2020.00695.
Tkhilaishvili, T., Di Luca, M., Abbandonato, G., Maiolo, E.M., Klatt, A.B., Reuter, M., Möncke-Buchner, E., Trampuz, A., 2018a. Real-time assessment of bacteriophage T3-derived antimicrobial activity against planktonic and biofilm-embedded Escherichia coli by isothermal microcalorimetry. Res. Microbiol. 169 (9), 515–521. https://doi.org/10.1016/j.resmic.2018.05.010.
Tkhilaishvili, T., Lombardi, L., Klatt, A.B., Trampuz, A., Di Luca, M., 2018b. Bacteriophage Sb-1 enhances antibiotic activity against biofilm, degrades exopolysaccharide matrix and targets persisters of Staphylococcus aureus. Int. J. Antimicrob. Agents 52 (6), 842–853. https://doi.org/10.1016/j.ijantimicag.2018.09.006.
Tkhilaishvili, T., Di Luca, M., Trampuz, A., 2018c. Simultaneous and sequential applications of phages and ciprofloxacin in killing mixed-species biofilm of Pseudomonas aeruginosa and Staphylococcus aureus. Orthopaed. Proc. 100. SUPP_1765-65The British Editorial Society of Bone & Joint Surgery.
Toinon, A., Greco, F., Moreno, N., Claire Nicolai, M., Guinet-Morlot, F., Manin, C., Ronzon, F., 2015. Study of rabies virus by Differential Scanning Calorimetry. Biochem. Biophys. Rep. 4, 329–336. https://doi.org/10.1016/j.bbrep.2015.10.010.
Virudachalam, R., Harrington, M., Markley, J.L., 1985a. Thermal stability of cowpea mosaic virus components: differential scanning calorimetry studies. Virology 146 (1), 138–140. https://doi.org/10.1016/0042-6822(85)90060-1.
Virudachalam, R., Low, P.S., Argos, P., Markley, J.L., 1985b. Turnip yellow mosaic virus and its capsid have thermal stabilities with opposite pH dependence: studies by differential scanning calorimetry and 31P nuclear magnetic resonance spectroscopy. Virology 146 (2), 213–220. https://doi.org/10.1016/0042-6822(85)90005-4.
Von Bertalanffy, L., 1950. The theory of open systems in physics and biology. Science 111 (2872), 23–29. https://doi.org/10.1126/science.111.2872.23.
Von Bertalanffy, L., 1971. General System Theory: Foundations, Development, Applications. George Braziller Inc, New York, NY. ISBN-13: 978-0807604533.
Von Stockar, U. (2013a). Live cells as open non-equilibrium systems. In Urs von Stockar, ed., Biothermodynamics: The Role of Thermodynamics in Biochemical Engineering, Lausanne: EPFL Press, 475-534. https://doi.org/10.1201/b15428.
Von Stockar, U. (2013b). Biothermodynamics of live cells: energy dissipation and heat generation in cellular structures. In: Biothermodynamics: the role of thermodynamics in Biochemical Engineering, von Stockar, U., ed., Lausanne: EPFL Press, pp. 475-534. https://doi.org/10.1201/b15428.
von Stockar, U., Liu, J., 1999. Does microbial life always feed on negative entropy? Thermodynamic analysis of microbial growth. Biochim. Biophys. Acta 1412 (3), 191–211. https://doi.org/10.1016/s0005-2728(99)00065-1.
Vorobieva, N., Sanina, N., Vorontsov, V., Kostetsky, E., Mazeika, A., Tsybulsky, A., Kim, N., Shnyrov, V., 2014. On the possibility of lipid-induced regulation of conformation and immunogenicity of influenza a virus H1/N1 hemagglutinin as antigen of TI-complexes. J. Mol. Microbiol. Biotechnol. 24 (3), 202–209. https://doi.org/10.1159/000365053.
Wang, Q., Li, Z., Ho, J., Guo, Y., Yeh, A.Y., Mohri, H., Liu, M., Wang, M., Yu, J., Shah, J. G., Chang, J.Y., Herbas, F., Yin, M.T., Sobieszczyk, M.E., Sheng, Z., Liu, L., Ho, D.D., 2022. Resistance of SARS-CoV-2 omicron subvariant BA.4.6 to antibody neutralisation. Lancet. Infect. Dis. 22 (12), 1666–1668. https://doi.org/10.1016/S1473-3099(22)00694-6.
Wang, L., Tkhilaishvili, T., Trampuz, A., 2020a. Adjunctive use of phage Sb-1 in antibiotics enhances inhibitory biofilm growth activity versus rifampin-resistant staphylococcus aureus strains. Antibiotics 9 (11), 749. https://doi.org/10.3390/antibiotics9110749. MDPI AG. Retrieved from.
Wang, L., Tkhilaishvili, T., Trampuz, A., Gonzalez Moreno, M., 2020b. Evaluation of staphylococcal bacteriophage Sb-1 as an adjunctive agent to antibiotics against rifampin-resistant *Staphylococcus aureus* biofilms. Front. Microbiol. 11, 602057 https://doi.org/10.3389/fmicb.2020.602057.
Wang, L., Tkhilaishvili, T., Bernal Andres, B., Trampuz, A., Gonzalez Moreno, M., 2020c. Bacteriophage-antibiotic combinations against ciprofloxacin/ceftriaxone-resistant Escherichia coli in vitro and in an experimental Galleria mellonella model. Int. J. Antimicrob. Agents 56 (6), 106200. https://doi.org/10.1016/j.ijantimicag.2020.106200.
Wang, G., Wang, H.J., Zhou, H., Nian, Q.G., Song, Z., Deng, Y.Q., Wang, X., Zhu, S.Y., Li, X.F., Qin, C.F., Tang, R., 2015. Hydrated silica exterior produced by biomimetic silicification confers viral vaccine heat-resistance. ACS Nano 9 (1), 799–808. https://doi.org/10.1021/nn5063276.
WHO (2022). WHO Coronavirus (COVID-19) Dashboard [Online] World Health Organization. Available at: https://covid19.who.int/(Accessed on January 5, 2023).
Wimmer, E., 2006. The test-tube synthesis of a chemical called poliovirus. The simple synthesis of a virus has far-reaching societal implications. EMBO Rep. S3–S9. https://doi.org/10.1038/sj.embor.7400728. *7 Spec No*(Spec No).
Yang, Y., Song, Y., Lin, X., Li, S., Li, Z., Zhao, Q., Ma, G., Zhang, S., Su, Z., 2020. Mechanism of bio-macromolecule denaturation on solid-liquid surface of ion-exchange chromatographic media - A case study for inactivated foot-and-mouth disease virus. J. Chromatogr. B Analyt. Technol. Biomed. Life Sci. 1142, 122051 https://doi.org/10.1016/j.jchromb.2020.122051.
Yang, Y., Zhao, Q., Li, Z., Sun, L., Ma, G., Zhang, S., Su, Z., 2017. Stabilization study of inactivated foot and mouth disease virus vaccine by size-exclusion HPLC and differential scanning calorimetry. Vaccine 35 (18), 2413–2419. https://doi.org/10.1016/j.vaccine.2017.03.037.

Yilmaz, B., Ercan, S., Akduman, S., Özilgen, M., 2020. Energetic and exergetic costs of COVID-19 infection on the body of a patient. Int. J. Exergy 32 (3), 314–327. https://doi.org/10.1504/IJEX.2020.10030515.

Yu, M., Zhang, S., Zhang, Y., Yang, Y., Ma, G., Su, Z., 2015. Microcalorimetric study of adsorption and disassembling of virus-like particles on anion exchange chromatography media. J. Chromatogr. A 1388, 195–206. https://doi.org/10.1016/j.chroma.2015.02.048.

Zhou, J., Rong, X.L., Cao, X., Tang, Q., Liu, D., Jin, Y.H., Shi, X.X., Zhong, M., Zhao, Y., Yang, Y., 2022. Assembly of poly(ethylene glycol)ylated oleanolic acid on a linear polymer as a pseudomucin for influenza virus inhibition and adsorption. Biomacromolecules 23 (8), 3213–3221. https://doi.org/10.1021/acs.biomac.2c00314.